Simulating the Generalized Gibbs Ensemble (GGE): a Hilbert space Monte Carlo approach

Vincenzo Alba[1]

[1]*International School for Advanced Studies (SISSA), Via Bonomea 265, 34136, Trieste, Italy, INFN, Sezione di Trieste*

(Dated: August 10, 2015)

By combining *classical* Monte Carlo and Bethe ansatz techniques we devise a numerical method to construct the Truncated Generalized Gibbs Ensemble (TGGE) for the spin-$\frac{1}{2}$ isotropic Heisenberg (XXX) chain. The key idea is to sample the Hilbert space of the model with the appropriate GGE probability measure. The method can be extended to other integrable systems, such as the Lieb-Liniger model. We benchmark the approach focusing on GGE expectation values of several local observables. As finite-size effects decay exponentially with system size, moderately large chains are sufficient to extract thermodynamic quantities. The Monte Carlo results are in agreement with both the Thermodynamic Bethe Ansatz (TBA) and the Quantum Transfer Matrix approach (QTM). Remarkably, it is possible to extract in a simple way the steady-state Bethe-Gaudin-Takahashi (BGT) roots distributions, which encode complete information about the GGE expectation values in the thermodynamic limit. Finally, it is straightforward to simulate extensions of the GGE, in which, besides the local integral of motion (local charges), one includes *arbitrary* functions of the BGT roots. As an example, we include in the GGE the first non-trivial quasi-local integral of motion.

Introduction.— The issue of how statistical ensembles arise from the out-of-equilibrium dynamics in *isolated* quantum many-body system is a fundamental, yet challenging, problem. The motivation for the interest in this topic is the degree of control reached in out-of-equilibrium experiments with cold atoms[1–15]. The paradigm experiment is the so-called global *quantum quench*[16], in which a system is initially prepared in an eigenstate $|\Psi_0\rangle$ of a many-body Hamiltonian $\mathcal{H}$. Then a global parameter of $\mathcal{H}$ is suddenly changed, and the system evolves under the new Hamiltonian $\mathcal{H}'$. At long times after the quench a steady state is reached, as confirmed by experiments[3]. In integrable models non-trivial *local* conserved quantities, besides the energy, strongly affects the dynamics and the nature of the steady state. As for now, despite the tremendous theoretical effort[17–56], it is unclear wheather such steady-state can be described by a statistical ensemble, and how to construct it.

It has been proposed that the stationary value of a generic local operator $\mathcal{O}$ is described by a Generalized Gibbs Ensemble[18,22] (GGE) as $\langle\mathcal{O}\rangle \equiv \mathrm{Tr}(\mathcal{O}\rho^{GGE})$. Here ρ^{GGE} extends the Gibbs density matrix by including all the extra conserved quantities $\mathcal{I}_j$ (charges) as

$$\rho^{GGE} = Z^{-1}\exp\big(-\lambda_j\mathcal{I}_j\big). \tag{1}$$

In (1), and in the following, repeated indices are summed over. Z is a normalization. The λ_j are Lagrange multipliers to be fixed by imposing $\langle\Psi_0|\mathcal{I}_j|\Psi_0\rangle = \langle\mathcal{I}_j\rangle$, and $\mathcal{I}_2 = \mathcal{H}'$ is the Hamiltonian. In realistic situations one deals with the truncated GGE[46] (TGGE), i.e., considering only the "most local" charges.

While the validity of the GGE has been confirmed in non-interacting theories[35,37,46,57,58], in interacting ones the scenario is less clear (see Ref. 48 for numerical results in an interacting model). For Bethe ansatz solvable models the Quench Action method[44] allows for an exact treatement of the steady state, provided that the overlap between the initial state $|\Psi_0\rangle$ and the eigenstates of $\mathcal{H}'$ are known. In several cases the Quench Action is in disagreement with the TGGE[51,53–55], whereas it is supported by numerics[53]. Recently, in Ref. 56 it has been shown that it is possible to "repair" the GGE by including the quasi-local charges[59–61]. Remarkably, this repaired GGE is in perfect agreement with the Quench Action[56], confirming that the description of the steady state with the GGE is correct, provided that the appropriate set of charges is considered. Note that the importance of quasi-local charges to construct the GGE in quantum field theories has been pointed out recently in Ref. 62 and Ref. 63.

On the other hand, numerical methods, such as the time dependent density matrix renormalization group[64,65] (tDMRG), have been mostly used to simulate the post-quench dynamics. However, no numerical attempt to explore the GGE *per se* has been undertaken yet. Our aim is to provide a Monte-Carlo-based framework for studying the GGE, and possible extensions, in exactly solvable models. We restrict ourselves to finite-size systems. We anticipate that, as finite-size corrections decay exponentially with system size[66], moderately large systems are sufficient to access the thermodynamic limit. The method relies on the knowledge of the Hilbert space structure provided by the Bethe ansatz, and on the Bethe-Gaudin-Takahashi (BGT) equations[67,68]. The key idea is the sampling of the Hilbert space according to the GGE probability measure (1). Note that the same idea has been already explored in Ref. 69 for the Gibbs ensemble. The method allows one to obtain GGE expectation value for generic observables, provided that their expression in terms of the roots of the BGT equations are known. It is also possible to extract the steady-state roots distributions, which encode the complete information about the GGE. It is also straightforward to extend the GGE including in (1) arbitrary functions of the BGT roots. This could be useful to investigate the effects of quasi-local charges. Finally, we should mention that, GGE averages can be computed using exact diagonalization or Quantum Monte Carlo. However, both these methods require the operatorial expression of the charges (see Ref. 70 for the XXX chain), whereas our results rely only on their expression (typically simple) in terms of the BGT roots.

We benchmark the approach focusing on the spin-$\frac{1}{2}$ isotropic Heisenberg (XXX) chain, which is the venerable prototype of integrable models[71]. We consider several

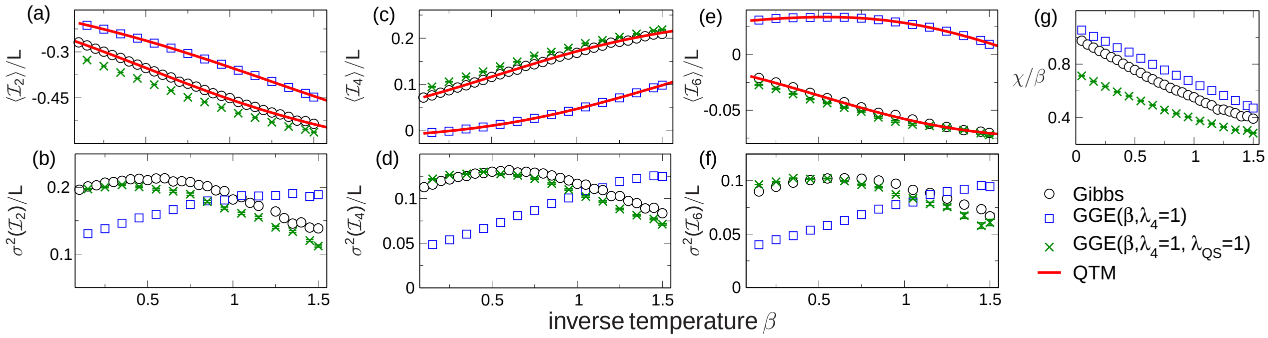

FIG. 1. The Generalized Gibbs Ensemble (GGE) for the XXX with $L = 16$ sites: Numerical results obtained using the Monte Carlo approach. Only the first two even conserved charges $\mathcal{I}_2, \mathcal{I}_4$ and the first quasi-local one $\mathcal{I}_{QS}$ are included in the GGE. $\mathcal{I}_2$ is the Hamiltonian. In all the panels the different symbols correspond to different values of the Lagrange multipliers λ_4, λ_{QS}. The circles denote the Gibbs ensemble, i.e., $\lambda_4 = \lambda_{QS} = 0$. The x-axis shows the inverse temperature $\lambda_2 = \beta$. (a) The GGE average $\langle \mathcal{I}_2/L\rangle$. (b) Variance of the charge fluctuations $\sigma^2(\mathcal{I}_2)/L \equiv (\langle \mathcal{I}_2^2\rangle - \langle \mathcal{I}_2\rangle^2)/L$ as a function of β. (c)(d) and (e)(f): Same as in (a)(b) for $\mathcal{I}_4$ and $\mathcal{I}_6$, respectively. In all panels the lines are the Quantum Transfer Matrix (QTM) results. (g) χ/β plotted versus β, with χ the magnetic susceptibility per site.

TGGEs (cf. (1)) constructed including $\mathcal{I}_2, \mathcal{I}_4$, and the first of the recently discovered[56,61] quasi-local charges $\mathcal{I}_{QS}$ (H_1^2 in Ref. 56). We focus on the conserved charges averages $\langle \mathcal{I}_j/L\rangle$, and on their fluctuations $\sigma^2(\mathcal{I}_j) \equiv \langle \mathcal{I}_j^2\rangle - \langle \mathcal{I}_j\rangle^2$, which are related to well-known observables, such as the energy density, and the specific heat. We also compute the spin susceptibility per site χ. Already for a chain with $L = 16$ sites the Monte Carlo data perfectly agree with both the standard Thermodynamic Bethe Ansatz[72] (TBA) and the Quantum Transfer Matrix approach[45,73] (QTM). Note that this is the first direct numerical verification of the QTM approach in the XXX chain. Finally, we extract the BGT roots distributions for both the Gibbs ensemble and the GGE. In both cases the finite-size effects are negligible for small roots, which are the relevant ones to describe the long-wavelength physics. For the Gibbs ensemble we compare our numerical data with standard finite-temperature Thermodynamic Bethe Ansatz (TBA) results, finding excellent agreement.

The-Heisenberg-spin-chain.— The XXX chain with L sites is defined by the Hamiltonian

$$\mathcal{H} \equiv J\sum_{i=1}^{L}\left[\frac{1}{2}(S_i^+S_{i+1}^- + S_i^-S_{i+1}^+) + S_i^zS_{i+1}^z - \frac{1}{4}\right], \quad (2)$$

where $S_i^{\pm} \equiv (\sigma_i^x \pm i\sigma_i^y)/2$ are spin operators acting on the site i, $S_i^z \equiv \sigma_i^z/2$, and $\sigma_i^{x,y,z}$ the Pauli matrices. We fix $J = 1$ and use periodic boundary conditions. The total magnetization $S_T^z \equiv \sum_i S_i^z = L/2 - M$, with M number of down spins, commutes with (2), and it is used to label its eigenstates.

In the Bethe ansatz each eigenstate of (2) is identified by M parameters $\{x_\alpha \in \mathbb{C}\}_{\alpha=1}^{M}$. In the limit $L \to \infty$ they form "string" patterns along the imaginary axis of the complex plane (string hypothesis[68,71]). Strings of length $1 \leq n \leq M$ (so-called n-strings) are parametrized as $x_{n;\gamma}^{j} = x_{n;\gamma} - i(n-1-2j)$. Here $x_{n;\gamma} \in \mathbb{R}$ is the string centers, $j = 0, 1, \dots, n-1$ labels different string components, and γ denotes different string centers. The string hypothesis is not correct for finite chains, although deviations typically decay exponentially with L. The $\{x_{n;\gamma}\}$ are obtained by solving the Bethe-Gaudin-Takahashi (BGT) equations[67,68]

$$L\vartheta_n(x_{n;\gamma}) = 2\pi I_{n;\gamma} + \sum_{(m,\beta)\neq(n,\gamma)} \Theta_{m,n}(x_{n;\gamma} - x_{m;\beta}). \quad (3)$$

Here $\vartheta_n(x) \equiv 2\arctan(x/n)$, $\Theta_{m,n}(x)$ is the scattering phase between different roots[68], and $I_{n;\gamma} \in \frac{1}{2}\mathbb{Z}$ the Bethe-Gaudin-Takahashi quantum numbers. The $I_{n;\gamma}$ satisfy the upper bound $|I_{n;\gamma}| \leq I_{\mathrm{MAX}}(n, L, M)$, with I_{MAX} a known function[68] of n, L, M. Every choice of $I_{n;\gamma}$ identifies an eigenstate of (2). We define the "string content" of each eigenstate as $\mathcal{S} \equiv \{s_1, \dots, s_M\}$, with $0 \leq s_n \leq \lfloor M/n \rfloor$ the number of n-strings. The local conserved charges $\mathcal{I}_j$ of the XXX chain are given as

$$\mathcal{I}_{j+1} \equiv \frac{i}{(j-1)!}\frac{d^j}{dy^j}\log\Lambda(y)\Big|_{y=i}, \quad (4)$$

where $\Lambda(y)$ is the eigenvalue of the quantum transfer matrix[74], with y a parameter. $\mathcal{I}_2$ is the XXX Hamiltonian. The support of $\mathcal{I}_j$, i.e., the number of adjacent sites where $\mathcal{I}_j$ acts non trivially, increases linearly with j, i.e., larger j correspond to less local charges. The eigenvalues of $\mathcal{I}_j$ on a generic eigenstate are obtained by summing the contributions of the different BGT roots *independently*. For instance, the energy eigenvalue is obtained as $E = 2\sum_{n,\gamma} n/(n^2 + x_{n;\gamma}^2)$. A similar result holds for the quasi-local charges[56].

The-Hilbert-space-Monte-Carlo-sampling.— For a finite chain the GGE (cf. (1)) can be constructed by importance sampling[75] of the eigenstates of (2). One starts with an initial M-particle eigenstate, with string content $\mathcal{S} = \{s_1, \dots, s_M\}$, and quantum number configuration $\mathcal{C} = \{I_{n;\gamma}\}_{n=1}^{M}$ ($\gamma = 1, \dots, s_n$). The corresponding charges eigenvalues are $\{\mathcal{I}_j\}$. Then a new eigenstate is generated with a Monte Carlo scheme. Each Monte Carlo step (mcs) consists of three moves:

1. Choose a new particle number sector M', and string content $\mathcal{S}' \equiv \{s'_1, \dots, s'_{M'}\}$ with probability[76]

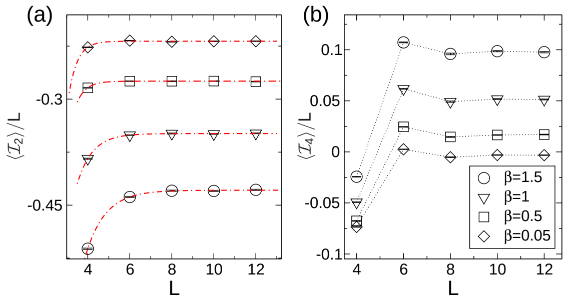

FIG. 2. Finite-size scaling of the GGE averages in the Heisenberg chain: Numerical results obtained from the Hilbert space Monte Carlo sampling. Here the GGE is constructed including $\mathcal{I}_2, \mathcal{I}_4$, with Lagrange multipliers $\lambda_2 = \beta, \lambda_4 = 1$. (a) $\langle \mathcal{I}_2/L \rangle$ plotted versus the chain size L for several values of β. The dash-dotted lines are exponential fits. (b) Same as in (a) for $\mathcal{I}_4$.

$\mathcal{P}(M', \mathcal{S}')$

$$\mathcal{P}(M', \mathcal{S}') = \frac{1}{B(L, L/2)} \prod_{i=1}^{M'} B\left(\mathcal{L}_i, \mathcal{S}'_i\right). \tag{5}$$

2. Generate a new quantum number configuration $\mathcal{C}'$ compatible with the $\mathcal{S}'$ obtained in step 1. Solve the corresponding BGT equations (3).

3. Calculate the charge eigenvalues $\mathcal{I}'_j$ and accept the new eigenstate with the Metropolis probability:

$$\mathrm{Min}\Big\{1, \frac{L - 2M' + 1}{L - 2M + 1} e^{-\lambda_j(\mathcal{I}'_j - \mathcal{I}_j)}\Big\}. \tag{6}$$

In (5) $B(x, y) \equiv x!/(y!(x-y)!)$ and $\mathcal{L}_i \equiv L - \sum_{j=1}^{M'} t_{ij} \mathcal{S}'_j$, with $t_{ij} \equiv 2\mathrm{Min}(i, j) - \delta_{ij}$. In (6) the factor in front of the exponential takes into account that $\mathcal{I}_j$ and the observables that we consider are invariant under $SU(2)$ rotations. Crucially, the steps 1 and 2 account for the density of states of the model, and are the same as for the Gibbs ensemble[69]. The iteration of 1-3 defines a Markov chain, which, after some thermalization steps, generates eigenstates distributed according to (1). Interestingly, by trivially modifying (6) it is possible to simulate GGE extensions in which, in addtion to $\mathcal{I}_j$, one considers arbitrary functions of the BGT roots. The GGE average $\langle \mathcal{O} \rangle$ of a generic operator is obtained as

$$\langle \mathcal{O} \rangle = \lim_{N_{\mathrm{mcs}} \to \infty} \frac{1}{N_{\mathrm{mcs}}} \sum_{|s\rangle} \langle s | \mathcal{O} | s \rangle, \tag{7}$$

where N_{mcs} is the total number of eigenstates $|s\rangle$ sampled. Moreover, for all the observables considered here the contributions of the BGT roots can be summed independently, i.e.,

$$\langle s | \mathcal{O} | s \rangle = \sum_{n,\gamma} f_{\mathcal{O}}(x_{n;\gamma}), \tag{8}$$

where the roots $x_{n;\gamma}$ identify the eigenstate $|s\rangle$, and $f_{\mathcal{O}}(x)$ depends on the observable.

The-GGE-for-local-observables.— The correctness of the Monte Carlo approach is illustrated in Fig. 1, considering the charge densities $\langle \mathcal{I}_j / L \rangle$ (panels (a)(c)(e) in the Figure), and the variance of their fluctuations $\sigma^2(\mathcal{I}_j)/L \equiv (\langle \mathcal{I}_j^2 \rangle - \langle \mathcal{I}_j \rangle^2)/L$ (panels (b)(d)(f)). Panel (g) plots χ/β, with χ the spin susceptibility. In all the panels the data correspond to the TGGE constructed with the first two even charges $\mathcal{I}_2, \mathcal{I}_4$, and the first non-trivial quasi-local charge $\mathcal{I}_{QS}$[56,61]. Different symbols correspond to different values of the associated Lagrange multipliers, namely $\lambda_4 = \lambda_{QS} = 0$ (Gibbs ensemble, circles in the Figure), $\lambda_4 = 1$ and $\lambda_{QS} = 0$ (squares), and $\lambda_4 = 0, \lambda_{QS} = 1$ (crosses). In all panels the x-axis shows the inverse temperature $\lambda_2 = \beta$. The data are Monte Carlo averages with $N_{\mathrm{mcs}} = 5 \cdot 10^5$ (cf. (7)). The continuous lines are the analyitic results in the thermodynamic limit obtained from the QTM approach. These fully match the Monte Carlo data, signaling that finite-size effects are negligible already for $L = 16$.

The finite-size corrections are more carefully investigated in Fig. 2, plotting $\langle \mathcal{I}_2 \rangle$ and $\langle \mathcal{I}_4 \rangle$ (panels (a) and (b), respectively) versus β. Clearly, finite-size effects decay exponentially[66] with L for any β. In (a) the dashed lines are fits to $c_1 + c_2 \exp(-c_3 L)$, with c_1, c_2, c_3 fitting parameters. Finite-size corrections are larger at lower temperature, and increase with the range of the operator (compare panels (a) and (b) in Fig. 2), as expected.

Extracting-the-root-distributions.— In the thermodynamic limit in each n-string sector the roots of (3) become dense. Thus, instead of the eigenstates, one considers the root distributions $\boldsymbol{\rho} \equiv \{\rho_n\}_{n=1}^{\infty}$, with $\rho_n \equiv \lim_{L\to\infty} [L(x_{n;\gamma+1} - x_{n;\gamma})]^{-1}$. The GGE average of an observable $\mathcal{O}$ becomes a functional integral as[72,77]

$$\mathrm{Tr}\{\exp\left(\lambda_j \mathcal{I}_j\right) \mathcal{O}\} \to \int \mathcal{D}\boldsymbol{\rho} \exp\left(S[\boldsymbol{\rho}] + \lambda_j \mathcal{I}_j[\boldsymbol{\rho}]\right) \mathcal{O}[\boldsymbol{\rho}]. \tag{9}$$

Here $S[\boldsymbol{\rho}]$ is the Yang-Yang entropy, which counts the number of eigenstates leading to the same $\boldsymbol{\rho}$ in the thermodynamic limit. In (9) we assume that $\mathcal{O}$ becomes a smooth functional of $\boldsymbol{\rho}$ in the thermodynamic limit. Eq. (8) becomes

$$\langle s | \mathcal{O} | s \rangle \to \sum_n \int dx \rho_n(x) f_{\mathcal{O}}(x). \tag{10}$$

Since both $S[\boldsymbol{\rho}]$ and $\mathcal{I}_j[\boldsymbol{\rho}]$ are extensive, the functional integral in (9) is dominated by the saddle point[72] $\boldsymbol{\rho}^{sp}$, with $\delta(S + \lambda_j \mathcal{I}_j)/\delta\boldsymbol{\rho}|_{\boldsymbol{\rho}=\boldsymbol{\rho}^{sp}} = 0$. Here $\boldsymbol{\rho}^{sp}$ acts as a representative state of the ensemble, and it contains the full information about the GGE. Eq. (7) and (10) imply that in the thermodynamic limit the histograms of the BGT roots sampled in the Monte Carlo converge to $\boldsymbol{\rho}^{sp}$.

This is numerically supported in Fig. 3. Panels (a)-(c) plot the root distributions $\rho_n^{sp}(x)$ for $n = 1, 2, 3$ as a function of x for the representative state (saddle point) of the infinite-temperature Gibbs ensemble. In each panel the different histograms correspond to different chain sizes $18 \le L \le 30$. The width of the histogram bins is varied with L as $2/L$. The full lines are the analytical Thermodynamic Bethe Ansatz[68] (TBA) results. Clearly, deviations from the TBA vanish upon

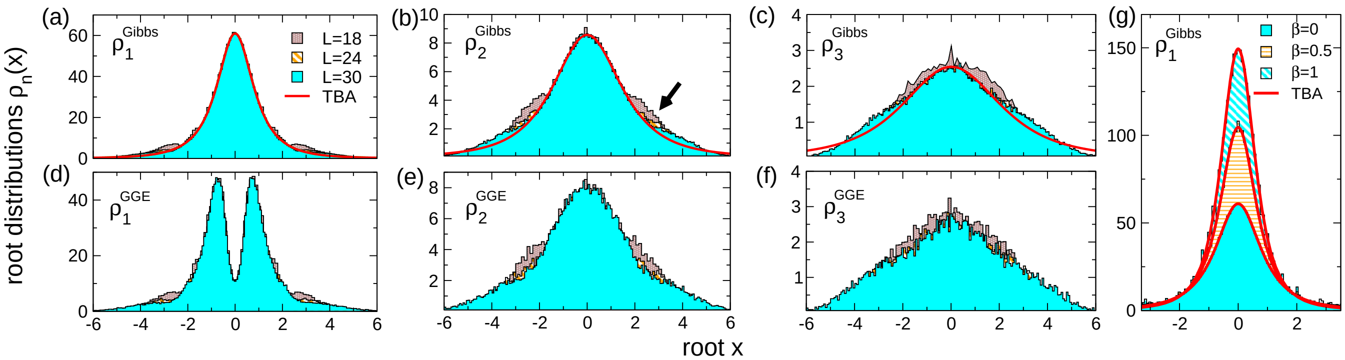

FIG. 3. The root distributions $\rho_n(x)$ (for $n = 1, 2, 3$) for the infinite temperature Gibbs (panels (a)-(c)) and the GGE equilibrium states (panels (d)-(f)): Numerical results for the Heisenberg spin chain obtained using the Hilbert space Monte Carlo sampling. Here the GGE is constructed including only $\mathcal{I}_2$ and $\mathcal{I}_4$ with fixed Lagrange multipliers $\lambda_2 = 0$ and $\lambda_4 = 1$. In all the panels the data are the histograms of the n-strings roots sampled in the Monte Carlo. The width of the histogram bins is $\Delta x = 2/L$, with L the chain size. In each panel different histograms correspond to different L. All the data are divided by 10^3 for convenience. In (b) the arrow highlights the finite-size effects. In (a)-(c) the lines are the Thermodynamic Bethe Ansatz (TBA) results. (g) Finite-temperature effects: Monte Carlo data for ρ_1^{Gibbs} for different values of the inverse temperature β.

increasing the chain size (see for instance the arrow in panel (b)). Moreover, the corrections are larger on the tails of the distributions. This is expected since large roots correspond to large quasi-momenta, which are more sensitive to the lattice effects. Finally, finite-size effects increase with n, i.e., with the bound state sizes, as expected. The results for the finite-temperature Gibbs ensemble are reported in Fig. 1 (g), for $\beta = 1/2$ and $\beta = 1$. We focus on $\rho_1^{sp}(x)$, considering $L = 30$. The infinite temperature histogram is reported for comparison. The lines are now finite-temperature TBA results, and perfectly agree with the Monte Carlo data. Upon lowering the temperature the height of the peak at $x = 0$ increases. This reflects that at $\beta = \infty$ the tail of the root distributions vanish exponentially, whereas for $\beta = 0$ they are[68] $\sim 1/x^4$. Finally, panels (d)-(f) plot $\rho_n(x)$ for the TGGE constructed with $\mathcal{I}_2, \mathcal{I}_4$ at fixed $\lambda_2 = 0$, $\lambda_4 = 1$ and for $L = 30$. Interestingly, in contrast with the thermal case (see (a)), ρ_1^{sp} exhibits a double peak at small x. Similar to the thermal case ((a)-(c) in the Figure), the data suggest that for $L = 30$ finite-size effects are negligible, at least for $-2 \leq x \leq 2$.

Conclusions.— We presented a Monte-Carlo scheme for simulating the truncated Generalized Gibbs ensemble (TGGE) in finite-size integrable models. The key idea is the importance sampling of the model eigenstates using the GGE probability. The method relies on the Bethe ansatz formalism, and, in particular, on the Bethe-Gaudin-Takahashi (BGT) equations. The thermodynamic limit can be accessed by standard finite-size scaling analysis. For local quantities finite-size corrections decay exponentially with the system size. Remarkably, the method allows to extract the steady-steate BGT root distributions, which contain full information about the GGE. Finally, it is possible to simulate extensions of the GGE, in which one includes as conserved charges arbitrary functions of the BGT roots. We bechmarked the method focusing on the spin-$\frac{1}{2}$ XXX chain. We compared our results with the standard Thermodynamic Bethe ansatz and the Quantum Transfer Matrix approach, finding agreement. Finally, we simulated an extended GGE by including the first non-trivial quasi-local charge.

As an interesting research direction, it would be useful to generalize the method to simulate the GGE at fixed value of the conserved charges. This should be possible using the standard microcanonical Monte Carlo techniques that have been developed in lattice gauge theory[78] and in molecular dynamics simulations[79]. Finally, by including in (6) the overlaps $\log |\langle \Psi_0 | \Psi_j \rangle|$, with $|\Psi_0\rangle$ the pre-quench initial state, and $|\Psi_j\rangle$ the model eigenstates, it should be possible to simulate the Quench Action[80].

1. I. Bloch, J. Dalibard, and W. Zwerger, Rev. Mod. Phys. **80**, 885 (2008).
2. M. Greiner, O. Mandel, T. Hänsch, and I. Bloch, Nature (London) **419**, 51 (2002).
3. T. Kinoshita, T. Wenger, and D. S. Weiss, Nature (London) **440**, 900 (2008).
4. S. Hofferberth, I. Lesanovsky, B. Fischer, T. Schumm, and J. Schiedmayer, Nature (London) **449**, 324 (2007).
5. S. Trotzky, Y.-A. Chen, A. Flesch, I. P. McCulloch, U. Schollwöck, J. Eisert, and I. Bloch, Nature Phys. **8**, 325 (2012).
6. M. Gring, M. Kuhnert, T. Langen, T. Kitagawa, B. Rauer, M. Schreitl, I. Mazets, D. A. Smith, E. Demler, and J. Schmiedmayer, Science **337**, 6100 (2012).
7. M. Cheneau, P. Barmettler, D. Poletti, M. Endres, P. Schaua, T. Fukuhara, C. Gross, I. Bloch, C. Kollath, and S. Kuhr, Nature (London) **481**, 484 (2012).
8. U. Schneider, L. Hackeruller, J. P. Ronzheimer, S. Will, S. Braun, T. Best, I. Bloch, E. Demler, S. Mandt, D. Rasch, and A. Rosch, Nature Phys. **8**, 213 (2012).
9. M. Kuhnert, R. Geiger, T. Langen, M. Gring, B. Rauer, T. Kita-

gawa, E. Demler, D. Adu Smith, and J. Schmiedmayer, Phys. Rev. Lett. **110**, 090405 (2013).

[10] T. Langen, R. Geiger, M. Kuhnert, B. Rauer, and J. Schmiedmayer, Nature Phys. **9**, 640 (2013).

[11] F. Meinert, M. J. Mark, E. Kirilov, K. Lauber, P. Weinmann, A. J. Daley, and H.-C. Nagerl, Phys. Rev. Lett. **111**, 053003 (2013).

[12] T. Fukuhara, A. Kantian, M. Endres, M. Cheneau, P. Schaua, S. Hild, C. Gross, U. Schollwöck, T. Giamarchi, I. Bloch, and S. Kuhr, Nature Phys. **9**, 235 (2013).

[13] J. P. Ronzheimer, M. Schreiber, S. Braun, S. S. Hodgman, S. Langer, I. P. McCulloch, F. Heidrich-Meisner, I. Bloch, and U. Schneider, Phys. Rev. Lett. **110**, 205301 (2013).

[14] S. Braun, M. Friesdorf, S. Hodgman, M. Schreiber, J. Ronzheimer, A. Riera, M. del Rey, I. Bloch, J. Eisert, and U. Schneider, PNAS **112**, 3641 (2015).

[15] T. Langen, S. Erne, R. Geiger, B. Rauer, T. Schweigier, M. Kuhnert, W. Rohringer, I. E. Mazets, T. Gasenzer, J. Schmiedmayer, Science **348**, 6231 (2015).

[16] A. Polkovnikov, K. Sengupta, A Silva, and M. Vengalattore, Rev. Mod. Phys. **83**, 863 (2011).

[17] P. Calabrese and J. Cardy, Phys. Rev. Lett. **96**, 136801 (2006).

[18] M. Rigol, V. Dunjko, V. Yurovsky, and M. Olshanii, Phys. Rev. Lett. **98**, 050405 (2007).

[19] P. Calabrese and J. Cardy, J. Stat. Mech. (2007) P06008.

[20] C. Kollath, A. M. Läuchli, and E. Altman, Phys. Rev. Lett. **98**, 180601 (2007).

[21] S. R. Manmana, S. Wessel, R. M. Noack, and A. Muramatsu, Phys. Rev. Lett. **98**, 210405 (2007).

[22] M. Rigol, V. Dunjko, and M. Olshanii, Nature **452**, 854 (2008).

[23] M. Cramer, C. M. Dawson, J. Eisert, and T. J. Osborne, Phys. Rev. Lett. **100**, 030602 (2008).

[24] T. Barthel and U. Schollwöck, Phys. Rev. Lett. **100**, 100601 (2008).

[25] M. Kollar and M. Eckstein, Phys. Rev. A **78**, 013626 (2008).

[26] M. Moeckel and S. Kehrein, Phys. Rev. Lett. **100**, 175702 (2008).

[27] A. Iucci and M. A. Cazalilla, Phys. Rev. A **80**, 063619 (2009).

[28] D. Rossini, A. Silva, G. Mussardo, and G. E. Santoro, Phys. Rev. Lett. **102**, 127204 (2009).

[29] P. Barmettler, M. Punk, V. Gritsev, E. Demler, and E. Altman, Phys. Rev. Lett. **102**, 130603 (2009).

[30] G. Biroli, C. Kollath, and A. M. Läuchli, Phys. Rev. Lett. **105**, 250401 (2010).

[31] D. Rossini, S. Suzuki, G. Mussardo, G. E. Santoro, and A. Silva, Phys. Rev. B **82**, 144302 (2010).

[32] D. Fioretto and G. Mussardo, New J. Phys. **12**, 055015 (2010).

[33] C. Gogolin, M. P. Mueller, and J. Eisert, Phys. Rev. Lett. **106**, 040401 (2011).

[34] M. C. Bañuls, J. I. Cirac, and M. B. Hastings, Phys. Rev. Lett. **106**, 050405 (2011).

[35] P. Calabrese, F. H. L. Essler, and M. Fagotti, Phys. Rev. Lett. **106**, 227203 (2011).

[36] M. Rigol and M. Fitzpatrick, Phys. Rev. A **84**, 033640 (2011).

[37] P. Calabrese, F. H. L. Essler, and M. Fagotti, J. Stat. Mech. (2012) P07016.

[38] J.-S. Caux and R. M. Konik, Phys. Rev. Lett. **109**, 175301 (2012).

[39] F. H. L. Essler, S. Evangelisti, and M. Fagotti, Phys. Rev. Lett. **109**, 247206 (2012).

[40] M. A. Cazalilla, A. Iucci, and M.-C. Chung, Phys. Rev. E **85**, 011133 (2012).

[41] J. Mossel and J.-S. Caux, New J. Phys. **14** 075006 (2012).

[42] M. Collura, S. Sotiriadis and P. Calabrese, Phys. Rev. Lett. **110**, 245301 (2013)

[43] G. Mussardo, Phys. Rev. Lett. **111**, 100401 (2013).

[44] J.-S. Caux and F. H. L. Essler, Phys. Rev. Lett. **110**, 257203 (2013).

[45] M. Fagotti and F. H. L. Essler, J. Stat. Mech. (2013), P07012.

[46] M. Fagotti and F. H. L. Essler, Phys. Rev. B **87**, 245107 (2013).

[47] S. Sotiriadis and P. Calabrese, J. Stat. Mech. (2014) P07024.

[48] M. Fagotti, M. Collura, F. H. L. Essler, and P. Calabrese, Phys. Rev. B **89**, 125101 (2014).

[49] F. H. L. Essler, S. Kehrein, S. R. Manmana, and N. J. Robinson, Phys. Rev. B **89**, 165104 (2014).

[50] G. Goldstein and N. Andrei, arXiv:1405.4224.

[51] J. De Nardis, B. Wouters, M. Brockmann, and J.-S. Caux, Phys. Rev. A **89**, 033601 (2014).

[52] T. M. Wright, M. Rigol, M. J. Davis, and K. V. Kheruntsyan, Phys. Rev. Lett. **113**, 050601 (2014).

[53] B. Pozsgay, M. Mestyán, M. A. Werner, M. Kormos, G. Zaránd, and G. Takács, Phys. Rev. Lett. **113**, 117203 (2014).

[54] B. Wouters, M. Brockmann, J. De Nardis, D. Fioretto, M. Rigol, and J.-S. Caux, Phys. Rev. Lett. **113**, 117202 (2014).

[55] M Mestyán, B. Pozsgay, G. Takács, and M. A. Werner, J. Stat. Mech. (2015) P04001.

[56] E. Ilieveski, J. De Nardis, B. Wouters, J.-S. Caux, F. H. Essler, and T. Prosen, arXiv:1507.02993.

[57] M. Kormos, M. Collura, and P. Calabrese, Phys. Rev. A **89**, 013609 (2014).

[58] P. P. Mazza, M. Collura, M. Kormos, and P. Calabrese, J. Stat. Mech. (2014) P11016.

[59] T. Prosen, Nucl. Phys. B **886**, (2014) 1177.

[60] R. G. Pereira, V. Pasquier, J. Sirker, and I. Affleck, J. Stat. Mech. (2014) P09037.

[61] E. Ilievski, M. Medejak, and T. Prosen, arXiv:1506.05049.

[62] F. H. L. Essler, G. Mussardo, and M. Panfil, Phys. Rev. A **91**, 051602 (2015).

[63] J. Cardy, arXiv:1507.07266.

[64] S. R. White and A. E. Feiguin, Phys. Rev. Lett. **93**, 076401 (2004).

[65] A. J. Daley, C. Kollath, U. Schollock, and G. Vidal, J. Stat. Mech. (2004) P04005.

[66] D. Iyer, M. Srednicki, and M. Rigol, Phys. Rev. E **91**, 062142 (2015).

[67] M. Takahashi, Prog. Theor. Phys. **46**, 401 (1971).

[68] M. Takahashi, *Thermodynamics of one-dimensional solvable models*, Cambridge University Press, Cambridge, 1999.

[69] S.-J. Gu, N. M. R. Peres, Y.-Q. Li, Eur. Phys. J. B **48**, 157 (2005).

[70] M. P. Grabowski and P. Mathieu, Ann. Phys. N.Y. **243**, 299 (1995).

[71] H. Bethe, Z. Phys. **71**, 205 (1931).

[72] J. Mossel and J.-S. Caux, J. Phys. A: Math. Theor. **45**, 255001 (2012).

[73] B. Pozsgay, J. Stat. Mech. (2013) P07003.

[74] V. E. Korepin, N. M. Bogoliubov, and A. G. Izergin, *Quantum Inverse Scattering Methods and Correlation Functions*, Cambridge University Press, Cambridge, 1997.

[75] D. P. Landau and K. Binder, *A Guide to Monte Carlo Simulations in Statistical Physics*, Cambridge University Press, Cambridge, 2000.

[76] L. D. Faddeev, arXiv:9605187.

[77] C. N. Yang and C. P. Yang, J. Math. Phys. **10**, 1115 (1969).

[78] M. Creutz, Phys. Rev. Lett. **50**, 1411 (1983).

[79] R. Lustig, J. Chem. Phys. **109**, 8816 (1998).

[80] In preparation.